ARTICLES

Journal of Semiconductors
(2019) 40, 062001
doi: 10.1088/1674-4926/40/6/062001

Growth of oxidation-resistive silicene-like thin flakes and Si nanostructures on graphene

Naili Yue[1], Joshua Myers[2], Liqin Su[1], Wentao Wang[3], Fude Liu[3], Raphael Tsu[1], Yan Zhuang[2], and Yong Zhang[1, †]

[1]Department of Electrical and Computer Engineering, The University of North Carolina at Charlotte, Charlotte, North Carolina 28223, USA

[2]Department of Electrical Engineering, Wright State University, Dayton, OH 45435, USA

[3]Department of Mechanical Engineering, The University of Hong Kong, Hong Kong, China

Abstract: We report the growth of Si nanostructures, either as thin films or nanoparticles, on graphene substrates. The Si nanostructures are shown to be single crystalline, air stable and oxidation resistive, as indicated by the observation of a single crystalline Si Raman mode at around 520 cm^{-1}, a STM image of an ordered surface structure under ambient condition, and a Schottky junction with graphite. Ultra-thin silicon regions exhibit silicene-like behavior, including a Raman mode at around 550 cm^{-1}, a triangular lattice structure in STM that has distinctly different lattice spacing from that of either graphene or thicker Si, and metallic conductivity of up to 500 times higher than that of graphite. This work suggests a bottom-up approach to forming a Si nanostructure array on a large-scale patterned graphene substrate that can be used to fabricate nanoscale Si electronic devices.

Key words: silicene; silicon; Raman; STM; epitaxial growth; oxidation

Citation: N L Yue, J Myers, L Q Su, W T Wang, F D Liu, R Tsu, Y Zhuang, and Y Zhang, Growth of oxidation-resistive silicene-like thin flakes and Si nanostructures on graphene[J]. *J. Semicond.*, 2019, 40(6), 062001. http://doi.org/10.1088/1674-4926/40/6/062001

1. Introduction

Since it was first pointed out in 2007 that silicene should have key electronic properties similar to those of graphene[1], a great deal of interest has been generated in the growth of silicene. Metallic substrates, mostly Ag but also ZrB_2, are typically used for silicene growth. However, the silicene structures grown on these substrates have been found to be highly distorted from the ideal (theoretically predicted) low-buckled bilayer structure[2, 3] and are unstable in air[4]. The severe structural distortion drastically shifts the silicene Raman frequency from theoretically predicted 562 cm^{-1}[5] or 575 cm^{-1}[6] of the ideal structure to around 520 cm^{-1}, which is nearly the same as the bulk Si[4, 7–9]. This situation is in stark contrast with that in a graphene-related structure: no matter how much structure distortion is exhibited in graphene, the sp^2 bonding related G peak at ~1600 cm^{-1} always persists despite the appearance of the sp^3 bonding related D peak at ~1300 cm^{-1}[10]. Meanwhile, in all of the reported cases of silicene, no Raman mode has been found at a frequency close to the predicted value. Additionally, the air stability of silicene is still a critical issue for this new material if it is to be practically useful. A multi-layer silicene (up to 43 monolayers) grown on Ag has been found to be more stable than a monolayer, but it still only lasts for up to 24 h[11]. Here, we report the MBE growth of single crystalline (ultra-) thin Si films on graphene. In the ultra-thin region, for the first time, we observe a Raman mode at ~550 cm^{-1}, which is very close to that of the free-standing silicene. More significantly, we find that the obtained Si structures remain intact, even 2–3 years after they were grown. This indicates that graphene is unique in serving as an anti-oxidation substrate.

The feasibility of growing silicene on graphene is supported by a few theoretical modeling results: DFT calculations show that the inter-layer binding between silicene and graphene is stronger than the interlayer–layer bonding of graphene layers in graphite[12]; molecular dynamics (MD) simulations indicate that a small Si cluster prefers to form a commensurate monolayer Si raft on the graphite surface[13], and DFT calculations suggest that silicene structure is energetically more favorable than diamond structure for small Si clusters on graphene[14]. Furthermore, despite the well-known bond length disparity between C and Si structure, it has been predicted that silicene and graphene could form a commensurate (i.e., nearly lattice matched) heterostrcture in $\sqrt{3}$x$\sqrt{3}$R30 stacking with respect to graphene because of the unique relationship in their bond lengths $d_{Si-Si} \approx \sqrt{3}d_{C-C}$[12, 15]. The graphene-like silicon structure can be viewed as a partially collapsed Si (111) monolayer with its bi-layer separation reduced from $d_{Si-Si}/3$ in the 3D structure to about one half of that in the ideal silicene[16, 17]. Graphene as a substrate is least likely to buckle due to its strong in-plane σ-bonding, and is thus less likely to distort the silicene structure. However, its π electrons can be used to facilitate a weak bonding with the epitaxial layer[18], and do not yet yield significant perturbation to the electronic structure of the epilayer[12, 15, 19]. These considerations motivate the effort to grow silicene on graphene[12, 15, 18, 19]. Graphene has recently been explored as the substrate for epitaxial growth of MoS_2 and $MoSe_2$[20, 21] or a universal buffer layer to grow other semiconductor materials on any substrate without the constrain of lattice matching[18]. Growing Si on

Correspondence to: Y Zhang, Yong.Zhang@uncc.edu
Received 5 FEBRUARY 2019; Revised 1 MARCH 2019.

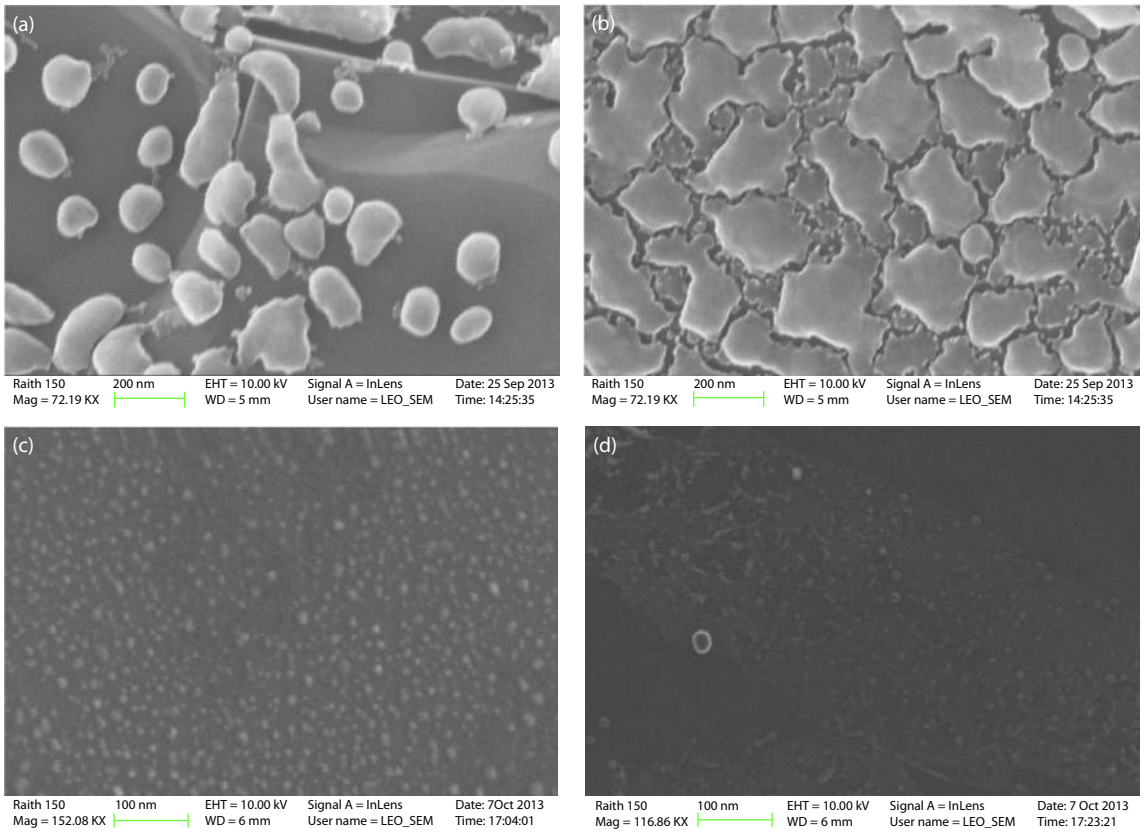

Fig. 1. SEM images of epitaxial silicon grown on graphite substrates. (a) and (b) from two areas on S1; (c) and (d) from two areas on S2.

graphite or graphene is also of interest to develop low cost Si photovoltaics[22] and also flexible Si electronics[23].

Before the recent interest in silicene, some efforts had already been made to grow Si on graphite, for instance, fullerene-structured Si nanowires[24], ultra-thin Si films[25], thick Si epilayers[26, 27], and Si nanocrystals[28]. However, these Si materials were often highly defective polycrystalline[26–28]. As expected for polycrystalline Si, the primary Si Raman mode near 520 cm^{-1} was found to be significantly broadened and red shifted[28]. Recently, ultra-thin silicon films deposited on highly oriented pyrolytic graphite (HOPG) and sapphire substrates were reported to exhibit sp^2-like bonding in photoemission studies[29], amorphous nano-Si structures have been coated on graphene and then used in Li-ion batteries[30], and silicene deposition on HOPG has been reported[19].

2. Experimental methods and results

In this work, thin Si films were grown on graphite and graphene on SiO_2/Si substrates in a MBE system (SVT Associates Inc.) by evaporating bulk Si with an e-beam evaporator. Graphite substrates of a few milimeters size were cleaved from a large single crystal of graphite. Si was deposited in the central region of the small graphite substrate. Since there is very little difference between a graphene and graphite when they are used as a substrate, graphite could be viewed as one layer of graphene supported by a large number of stacked graphene layers with weak bonding, similar to graphene on another supporting material, such as SiO_2. Therefore, we will refer to both graphite and graphene on SiO_2 as graphene substrate. The typical growth conditions are as follows: growth chamber base pressure being 2×10^{-8} Torr; heating the substrate to the growth temperature T_g = 800 or 850 °C and held for 15 min; e-beam evaporator running with acceleration voltage 6.07 kV, emission current 150 mA, and filament current 31 A; growth time t_g = 15 or 10 min; holding at T_g for 5 min; cooling rate 10 °C/min from T_g to 500 °C, then cooled down naturally to room temperature in the growth chamber.

Surface morphology was characterized by SEM and AFM. Si particles and thin-film-like structures were found to form on the cleaved graphite surface that exhibited various clean and flat regions more than 10 μm in size. These regions provide high quality single crystalline graphene to serve as template for epitaxial growth. Transferred graphene on other types of substrates is likely more defective, either due to the presence of polycrystalline domains or chemical residues associated with the transfer. A few typical SEM images are shown in Fig. 1. Figs. 1(a) and 1(b) were taken from sample S1 with T_g/t_g = 800 °C/15 min, showing two areas of different densities of Si particles or islands, roughly 100–200 nm in size. Figs. 1(c) and 1(d) from sample S2 with T_g/t_g = 850 °C/10 min, showing one area with very small Si particles in the order of 10 nm, and a thin-film like structure of a few μm in size, possibly with embedded small Si particles. The heights of these Si structures were found to be typically in the range of 1 to 15 nm measured by AFM, as shown in the two representative AFM images: Figs. 2(a) and 2(b). Another sample (S3) grown on a graphene/SiO_2/Si substrate was examined by TEM, which indicates that Si nanocrystals, typically a few nm in size, were observed on the surface. Fig. 2(c) is a low magnification image, showing Si layer deposited on the graphene/SiO_2 substrate. Fig. 2(d) is a high resolution image with visible Si lattice planes of a single Si nanocrystal, but the graphene layer is too thin to see.

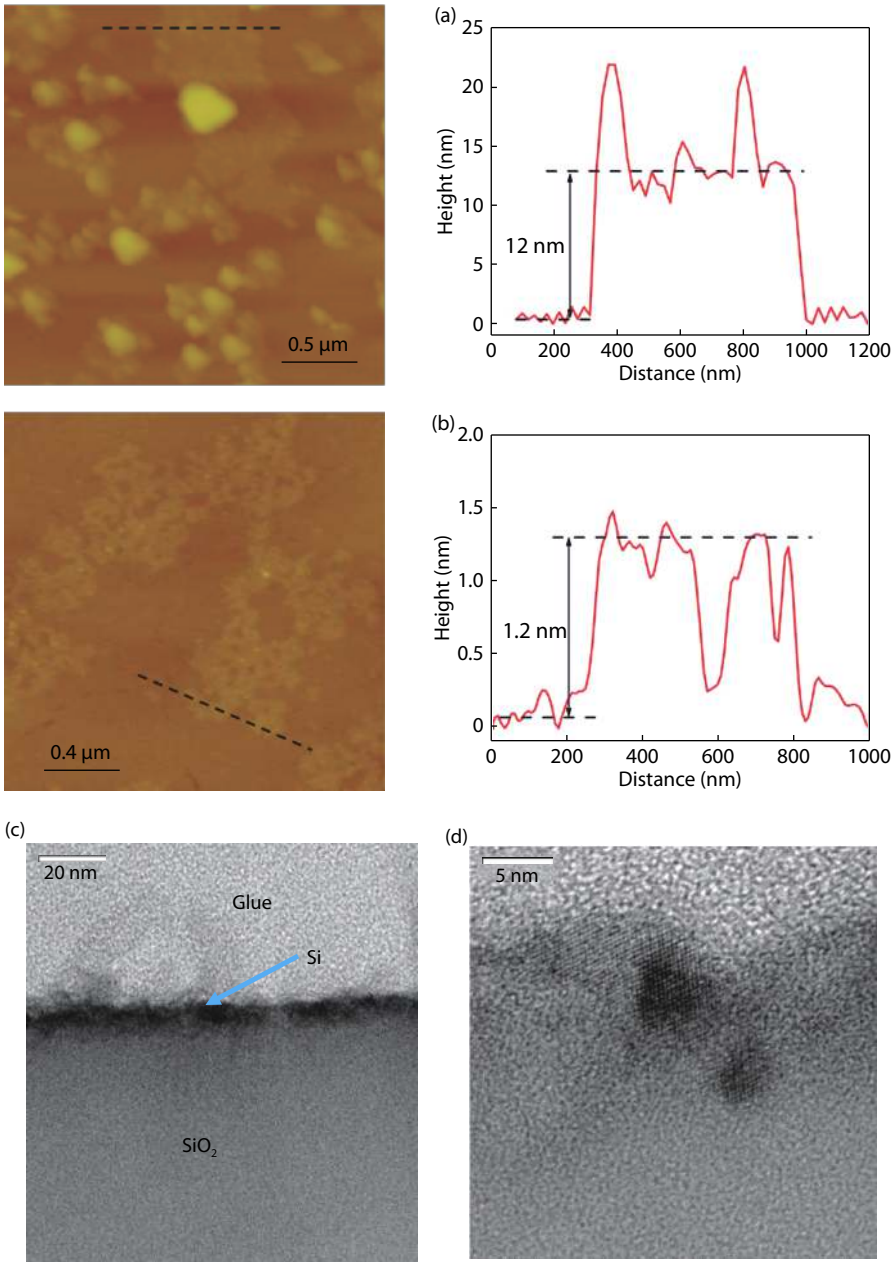

Fig. 2. (Color online) AFM and TEM images of epitaxial thin Si film grown on graphite and graphene. (a) and (b) AFM images from samples S1 and S2, respectively. (c) and (d) TEM images from sample S3.

The epitaxial Si structures were characterized by confocal microRaman using a Horiba LabRam HR800 Raman microscope with a 100× lens (NA = 0.9), excited with a 532 nm laser. A sufficiently low laser power (~ 1 mW) was used to minimize heating induced peak shift. Fig. 3 shows a few representative Raman spectra from the Si on graphite samples. Fig. 3(a) is from S1 measured on two areas: one with a Si particle and the other a uniform area, compared with a bulk Si. In contrast to the severely distorted Raman spectra reported for Si nanoparticles also grown on graphite[28], here we have observed single crystalline Si-like Raman spectra for the epitaxial Si structures with only a small redshift in the peak position and a small broadening in linewidth. Interestingly, the shift of the thin-film area is slightly more than a particle that is somewhat thicker. Note that despite the expected close lattice matching between graphene and Si (111), the in-plane lattice constant of Si is actually a few percent smaller. It has been documented that 2D films like monolayer MoS_2 and WS_2 usually form significant chemical bonding with the substrates on which they are grown[31–33]. Given the predicted weak but signifiant chemical bonding between graphene and silicene[12, 15], we expect that the thin diamond-like Si structure could experience some tensile epitaxial strain from the graphite substratete substrate[12, 15]. The strain could qualitatively explain the variation in redshift that is larger for the thinner layer. In addition, the expected nonuniform bond lengths along the growth direction, due to the variation of the in-plane lattice constant with the thickness, might also contribute to the small Raman line broadening. In terms of Raman intensity, if we assume that Raman signal is proportional to the sample volume, based on the absorption coefficient of Si ($\alpha \sim 10^4$ cm^{-1} at 532 nm), then we can offer a rough estimate for the Si film thickness to be 1.4 nm (i.e., 4–5 monolayers thick using the monolayer thickness of bulk Si at 3.15 Å). This estimate is consistent with what we meas-

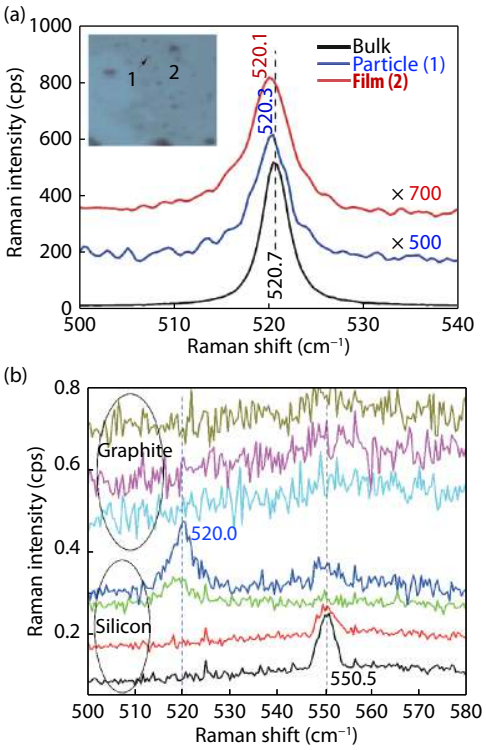

Fig. 3. (Color online) Raman spectra of epitaxial thin silicon on graphene. (a) Spectra from two sites on S1, compared with that of bulk Si. (b) Spectra from multiple sites of thin Si films, compared to graphite spectra (inset: an optical image of the area).

ured with AFM from the thin area, such as Fig. 2(b), although precise correlation between Raman signal intensity and film thickness, particularly down to a few monolayers, is usually not straightforward[34].

Based on the phonon frequency change between diamond F_{2g} mode (~1300 cm^{-1}) and graphene E_{2g} mode (~1600 cm^{-1}), one would expect that the silicene E_{2g} phonon frequency to be roughly in proportion higher than that of bulk Si at ~520 cm^{-1}. Indeed, the theoretically predicted value for free-standing silicene is 562 cm^{-1}[5] or 575 cm^{-1}[6]. Therefore, the spectra shown in Fig. 3(a) are likely to be bulk-like Si structures. However, at certain locations that appear to have ultra-thin Si films based on the signal strength, we have instead observed a Raman mode at 550.5 cm^{-1}, with a comparable linewidth of the bulk Si mode, as shown in Fig. 3(b) with spectra measured from multiple Si sites and graphite sites. On these Si sites, there is an anti-correlation between the 3D Si peaks near 520 cm^{-1} and the new Si related Raman mode near 550 cm^{-1}. This 550.5 cm^{-1} mode is much closer to the predicted free-standing silicene mode than previously reported silicene Raman modes that were very close to that of the bulk Si. The redshift from the theoretical value could be due to the presence of the tensile strain from the substrate[12, 15]. We note that these Si related spectra are distinctly different from those of graphite that do not exhibit any well defined feature in the same spectral range. SiO_2 could be another possible alternative for the origin of the new Raman mode. However, amorphous SiO_2 does not have any well-defined Raman peak near 550 cm^{-1}[35, 36].

It is unusual for the Raman spectra of these very thin Si samples to remain highly stable 2–3 years after the samples were grown. One would expect that such thin Si structures had been mostly oxidized and converted into SiO_2, given the oxidation rate of 11–13 Å in one day[37] or about 2 nm in one month[38]. This is an important indication of the anti-oxidation effect of the graphene substrate. However, a more intriging and convincing finding is offered by STM measurements done on one of the samples.

Fig. 4 shows the electrical characterization and STM images for three distinctly different regions on sample S1: of no Si growth (i.e., exposed graphite), of ultra-thin Si (i.e., area with silicene like behavior), and of relatively thick Si. These measurements were acquired using an Agilent AFM 5420 atomic force microscope with a STM nose cone and scanner. The tip was prepared by cutting the wire at a 45° angle prior to lowering into position. The current scans were performed in constant current mode and STM images were obtained in constant height mode. The *I–V* curves were taken by bringing the tip into contact with the sample at different selected locations of interest, where the tip was held at a constant position and a voltage sweep was performed while measuring the current. The surface of the graphite substrate away from the growth region was used as one contact, and the tip was grounded. Fig. 4(a) is the current map of an area with Si deposition, showing ribbon-like Si structures. The brownish colored area is graphite, the lightest colored area is the thicker Si, whereas the dark area between is the ultra-thin, silicene like Si; as judged by their *I–V* characteristics and STM images. Note that the strong current contrast revealed in Fig. 4(a) happens because of the very large variations in conductivity between the three regions such that, despite attempting to measure in the constant current mode, the system was unable to maintain a constant current. Fig. 4(b) contrasts the typical *I–V* characteristics of the three regions under the contact mode. The graphite region is least conductive, then comes the thicker Si region, and finally the silicene-like region is most conductive, with a conductivity of up to 500 times that of the graphite region. For instance, at 3.5 mV the current of the silicene-like region is 370 times that of the graphite region. Also, at ±0.5 V, our conductivity is about a factor of 10 larger than that in the previously reported silicene grown on graphite[19]. The high conductivity of the silicene-like region could be due to the charge transfer effect from graphite to silicene[15]. Figs. 4(c), 4(e), and 4(g) plot the *I–V* curves of the three regions in an extended voltage range, respectively. Both graphite and silicene-like regions show ohmic behavior though with large difference in conductivity, whereas the thicker Si exhibits Schottky junction type characteristic, consistent with literature reports for either graphite or graphene/bulk Si junctions[39–41]. The conductivity change with increasing film thickness is qualitatively consistent with the expectation that beyond two monolayers, the multi-layer silicene or thin-Si film becomes a semiconductor[42]. Figs. 4(d), 4(f), and 4(h) give the corresponding STM images obtained under ambient conditions from the three regions, respectively. They show distinctively different patterns. The pattern of Fig. 4(d) resembles that expected for graphite, which is a triangular lattice[43], although it is highly distorted, and the bright-spot separation of 2.40 ± 0.43 Å is in good agreement with the lattice constant of graphite at 2.46 Å. Although the topmost layer of graphite is a graphene layer with a hexagonal structure, the STM image should instead be a triangular lattice, due to the interference of the layer underneath[43, 44]. The patterns in

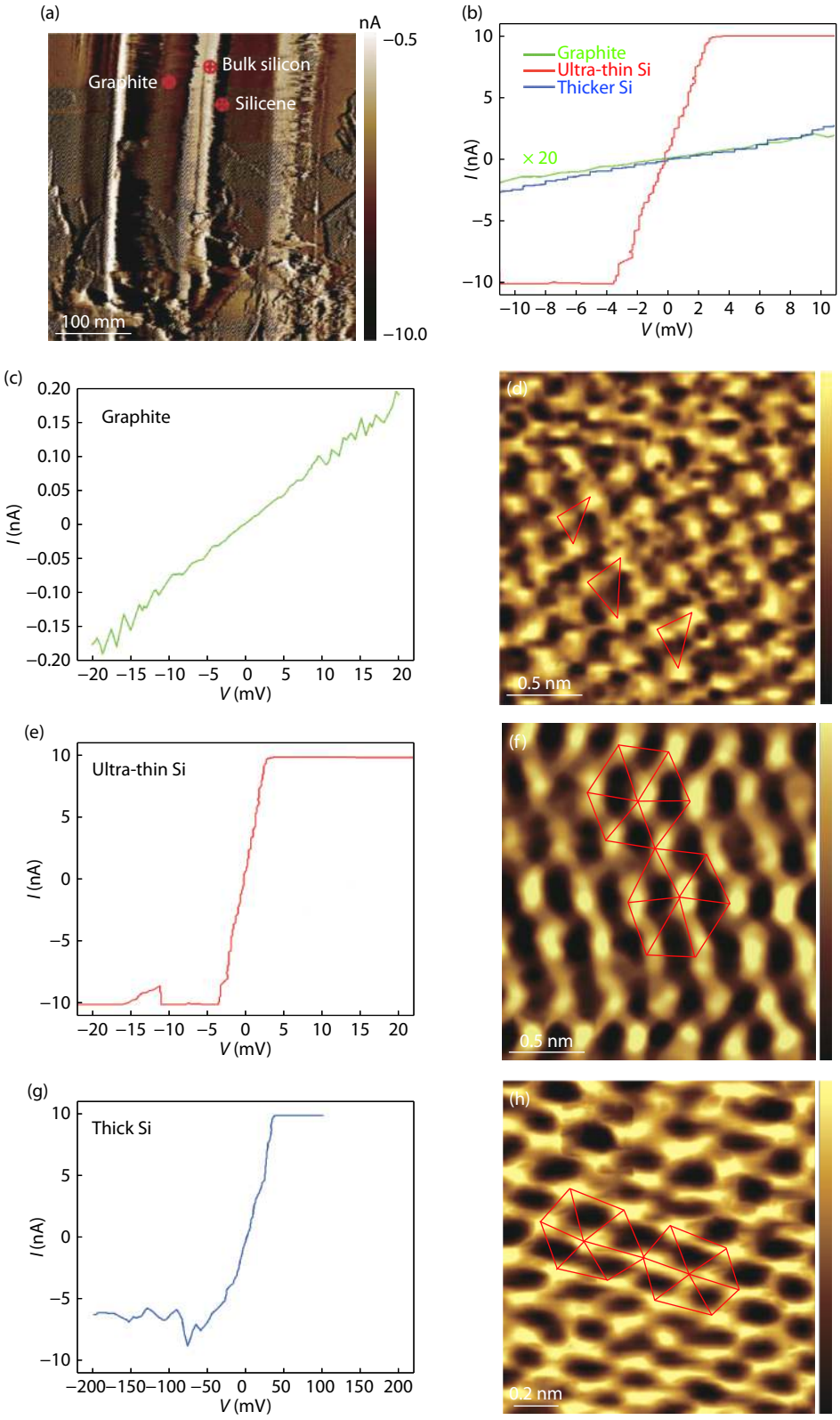

Fig. 4. (Color online) STM images and *I*–*V* curves of epitaxial thin silicon on graphite. (a) Current map over a large area containing three types of regions. (b) Comparison of *I*–*V* curves of the three types of regions under low bias voltages. (c) and (d) *I*–*V* curve and STM image of graphite. (e) and (f) *I*–*V* Curve and STM image of ultra-thin silicon. (g) and (h) *I*–*V* curve and STM image of thick silicon.

Figs. 4(f) and 4(h) for the Si areas are more regular—they both are triangular lattices but the spacings are quite different from each other and from that of the graphite region. In Fig. 4(f) for the silicene like Si, the pattern is consistent with what is expected for the Si version of graphite[43]. The bright-spot separations are 3.53 ± 0.19 Å, which are somewhat smaller than the silicene lattice constant (about 3.8 Å). The structure revealed by Fig. 4(h) for the thicker silicon region shows a bright-spot spacing of 1.93 ± 0.22 Å, which does not match any of the known reconstructed Si surfaces[45]. Nevertheless, it is a total surprise that one could observe the Si (111) by STM in air after the long air exposure of the sample (grown in December,

2011, and measured in August, 2013). While the exact underlying structures corresponding to these STM images remain to be confirmed through other means, the differentiations between them confirm that they exhibit distinctively different material properties.

3. Discussion

A freshly cleaved Si (111) surface will undergo surface reconstruction if kept in high vacuum, otherwise it will be oxidized into a SiO_2 capping layer. In either case, the surface modification is to remove the dangling bonds or minimize the surface energy. Besides SiO_2, hydrogen atoms are often used to passivate the dangling bonds in Si. These processes apply to a thick bulk Si. When the layer is sufficiently thin and electronically coupled to a substrate, charge transfer across the heterostructure interface may drastically change the picture. If a very thin Si slab remains in its idealistic sp^3 bonding, then it will have one dangling bond on the top layer and one on the bottom layer. There are at least two ways to mitigate the dangling bonds: (1) If the slab is only one monolayer thick, then partially collapsing the buckled (111) monolayer will allow the upper and lower dangling bonds to form a partial π bond, yielding the so-called silicene that is in-principle structurally stable, although it remains chemically unstable (because the weak partial π bond is susceptible to chemical reaction). In contrast, a fully collapsed diamond (111) monolayer forms a much stronger π bond, namely graphene, and thus is chemically much more stable. (2) Accepting charge from the substrate to passivate the dangling bonds, which has been shown to be theoretically possible for a silicene/graphene superlattice[15]. Charge transfer induced passivation has been demonstrated to yield stable inorganic-organic hybrid superlattices with two monolayer thick II–VI slabs in reality[46]. It requires more precise growth control and structure characterization to achieve and confirm the feasibility of growing a single layer silicene. However, a self-passivated ultra-thin Si film or multi-layer silicene could potentially be more useful for practical applications than monolayer silicene because it retains the basic properties of the Si, most importantly the bandgap[42], whereas silicene is metallic.

4. Summary

The ability to grow a single-crystalline thin Si film on graphene substrate opens up new avenues for future generation Si electronic devices. It is highly desirable for fabricating flexible Si based devices being able to perform either pre- or post-growth transfer of graphene or graphene with the grown Si structures to different substrates. Before a large and uniform graphene substrate is available, it might be challenging to grow a large and continuous thin Si film. However, it may not be necessary after all if the goal is to make nanoscale Si devices because a large film is only needed for the traditional top–down approach. This work suggests the possibility to selectively deposit high quality nanoscale Si structures: silicene, a-few-layer silicene, and Si nanocrystals, using a template of nanoscale graphene structures. For instance, one possible way to obtain such a template could be to first grow an array of SiC nanostructures on a large Si wafer and then convert them into graphene nanostructures with a laser beam[47], followed by the growth of Si nanostructures (as demonstrated in this work).

The exact epitaxial relationship between the epitaxial Si structures and the graphene layer is yet to be determined. This is largely true for the epitaxial growth on graphene in general. Si on graphene can provide a simpler model system for understanding the van der Waals epitaxy. We expect that this work will inspire future research and exploration in both applied and fundamental areas, such as semiconductor nanostructures and devices, surface science, and surface passivation.

Acknowledgement

The work at UNCC was supported by ARO/Materials Science (Grant No. W911NF-10-1-0281 and W911NF-18-1-0079, managed by Dr. Chakrapani Varanasi). We thank Dr. Weijie Lu for providing the single crystal graphite, Dr. Chun-Sheng Jiang for helpful discussions on STM, Drs. Kai Wang and Gerd J. Duscher for attempting to identify the epitaxial relationship between the substrate and Si structures. YZ acknowleges the support of Bissell Distinguished Professorship.

References

[1] Guzm-Verri G G, Lew Yan Voon L C. Electronic structure of silicon-based nanostructures. Phys Rev B, 2007, 76, 075131
[2] Vogt P, De Padova P, Quaresima C, et al. Silicene: compelling experimental evidence for graphenelike two-dimensional silicon. Phys Rev Lett, 2012, 108, 155501
[3] Fleurence A, Friedlein R, Ozaki T, et al. Experimental evidence for epitaxial silicene on diboride thin Films. Phys Rev Lett, 2012, 108, 245501
[4] Cinquanta E, Scalise E., Chiappe D, et al Getting through the nature of silicene: an sp2-sp3 two-dimensional silicon nanosheet. J Phys Chem C, 20113, 117, 16719
[5] Yan J A, Stein R, Schaefer D M, et al. Electron-phonon coupling in two-dimensional silicene and germanene. Phys Rev B, 2013, 88, 121403
[6] Scalise E, Houssa M, Pourtois G, et al. Vibrational properties of silicene and germanene. Nano Res, 2013, 6, 19
[7] Solonenko D, Gordan O, Lay G L, et al. 2D vibrational properties of epitaxial silicene on Ag(111). 2D Mater, 2017, 4, 015008
[8] Zhuang J, Xu X, Du Y, et al. Investigation of electron–phonon coupling in epitaxial silicene by in situ Raman spectroscopy. Phys Rev B, 2015, 91, 161409
[9] Sheng S, Wu J B, Cong X, et al. Vibrational properties of a monolayer silicene sheet studied by tip-enhanced Raman spectroscopy. Phys Rev Lett, 2017, 119, 196803
[10] Wu J B, Lin M L, Cong X, et al. Raman spectroscopy of graphene-based materials and its applications in related devices. Chem Soc Rev, 2018, 47, 1822
[11] De Padova P, Ottaviani C, Quaresima C, et al. 24 h stability of thick multilayer silicene in air. 2D Mater, 2014, 1, 021003
[12] Zhang Y, Tsu R. Binding graphene sheets together using silicon: graphene/silicon superlattice. Nanoscale Res Lett, 2010, 5, 805
[13] Neuendorf R, Palmer R E, Smith R. Low energy deposition of size-selected Si clusters onto graphite. Chem Phys Lett, 2001, 333, 304
[14] Cai Y, Chuu C P, Wei C M, et al. Stability and electronic properties of two-dimensional silicene and germanene on graphene. Phys Rev B, 2013, 88, 245408
[15] Yu S, Li X D, Wu S Q, et al. Novel electronic structures of superlattice composed of graphene and silicene. Mater Res Bull, 2014, 50, 268
[16] Fahy S, Louie S G, Cohen M L. Pseudopotential total-energy study of the transition from rhombohedral graphite to diamond. Phys Rev B, 1986, 34, 1191

[17] Wang J, Zhang Y. Topologic connection between 2-D layered structures and 3-D diamond structures for conventional semiconductors. Sci Rep, 2016, 6, 24660
[18] Zhang Y, Tsu R, Yue N. Growth of semiconductors on hetero-substrates using graphene as an interfacial layer. US Patent, US2014/039596, 2014
[19] De Crescenzi M, Berbezier I, Scarselli M, et al. Formation of silicene nanosheets on graphite. ACS Nano, 2016, 10, 11163
[20] Li Y, Wang H, Xie L, et al. MoS_2 nanoparticles grown on graphene: an advanced catalyst for the hydrogen evolution reaction. J Am Cheml Soc, 2011, 133, 7296
[21] Ugeda M M, Bradley A J, Shi S F, et al. Giant bandgap renormalization and excitonic effects in a monolayer transition metal dichalcogenide semiconductor. Nat Mater, 2014, 13, 1091
[22] Teplin C W, Paranthaman M P, Fanning T R, et al. Heteroepitaxial film crystal silicon on Al_2O_3: new route to inexpensive crystal silicon photovoltaics. Energy Environ Sci, 2011, 4, 3346
[23] Zhang K, Seo J H, Zhou W D, et al. Fast flexible electronics using transferrable silicon nanomembranes. J Phys D, 2012, 45, 143001
[24] Marsen B, Sattler K. Fullerene-structured nanowires of silicon. Phys Rev B, 1999, 60, 11593
[25] Nath K G, Shimoyama I, Sekiguchi T, et al. Chemical-state analysis for low-dimensional Si and Ge films on graphite. J Appl Phys, 2003, 94, 4583
[26] Kunze T, Hauttmann S, Seekamp J, et al. Recrystallized and epitaxially thickened poly-silicon layers on graphite substrates. Conference Record of the IEEE Photovoltaic Specialists Conference, 1997, 735
[27] Beaucarne G, Bourdais S, Slaoui A, et al. Impurity diffusion from uncoated foreign substrates during high temperature CVD for thin-film Si solar cells. Sol Energy Mater Sol Cells, 2000, 61, 301
[28] Wang L, Tu H L, Zhu S W, et al. Dispersed Si nanoparticles with narrow photoluminescence peak prepared by laser ablated deposition. Chin J Nonferrous Metals, 2010, 20, 724
[29] Baba Y, Shimoyama I, Hirao N, et al. Structure of ultra-thin silicon film on HOPG studied by polarization-dependence of X-ray absorption fine structure. Chem Phys Lett, 2014, 594, 64
[30] Evanoff K, Magasinski A, Yang J, et al. Nanosilicon-coated graphene granules as anodes for Li-ion batteries. Adv Energy Mater, 2011, 1, 495
[31] Su L, Zhang Y, Yu Y, et al. Dependence of coupling of quasi 2-D MoS_2 with substrates on substrate types, probed by temperature dependent Raman scattering. Nanoscale, 2014, 6, 4920
[32] Su L, Yu Y, Cao L, et al. Effects of substrate type and material-substrate bonding on high-temperature behavior of monolayer WS_2. Nano Res, 2015, 8, 2686
[33] Su L, Yu Y, Cao L, et al. In situ in situ monitoring of the thermal-annealing effect in a monolayer of MoS_2. Phys Rev Appl, 2017, 7, 034009
[34] Li L X, Han W P, Wu W. J B, et al Layer-number dependent optical properties of 2D materials and their application for thickness determination. Adv Funct Mater, 2017, 27, 1604468
[35] Malinovsky V K, Novikov V N, Surovtsev N V, et al. Investigation of amorphous states of SiO_2 by Raman scattering spectroscopy. Phys Solid State, 2000, 42, 65
[36] Ivanda M, Clasen R, Hornfeck M, et al. Raman spectroscopy on SiO_2 glasses sintered from nanosized particles. J Non-Cryst Solids, 2003, 322, 46
[37] Raider S I, Flitsch R, Palmer M J. Oxide growth on etched silicon in air at room temperature. J Electrochem Soc, 1975, 122, 413
[38] Ryckman J D, Reed R A, Weller R A, et al. Enhanced room temperature oxidation in silicon and porous silicon under 10 keV X-ray irradiation. J Appl Phys, 2010, 108, 113528
[39] Tongay S, Schumann T, Hebard A F. Graphite based Schottky diodes formed on Si, GaAs, and 4H-SiC substrates. Appl Phys Lett, 2009, 95, 222103
[40] Sinha D, Lee J U. Ideal graphene/silicon schottky junction diodes. Nano Lett, 2014, 14, 4660
[41] Riazimehr S, Schneider D, Yim C, et al. Spectral sensitivity of a graphene/silicon pn-junction photodetector. 2015 Joint International EUROSOI Workshop and International Conference on Ultimate Integration on Silicon, 2015, 77
[42] Guo Z X, Zhang Y Y, Xiang H, et al. Structural evolution and optoelectronic applications of multilayer silicene. Phys Rev B, 2015, 92, 201413
[43] Mizes H A, Park S I, Harrison W A. Multiple-tip interpretation of anomalous scanning-tunneling-microscopy images of layered materials. Phys Rev B, 1987, 36, 4491
[44] Hembacher S, Giessibl F J, Mannhart J, et al. Revealing the hidden atom in graphite by low-temperature atomic force microscopy. Proc Natl Acad Sci, 2003, 100, 12539
[45] Neddermeyer H. Scanning tunnelling microscopy of semiconductor surfaces. Rep Prog Phys, 1996, 59, 701
[46] Zhang Y, Dalpian G M, Fluegel B, et al. Novel approach to tuning the physical properties of organic-inorganic hybrid semiconductors. Phys Rev Lett, 2006, 96, 026405
[47] Yue N, Zhang Y, Tsu R. Ambient condition laser writing of graphene structures on polycrystalline SiC thin film deposited on Si wafer. Appl Phys Lett, 2013, 102, 071912